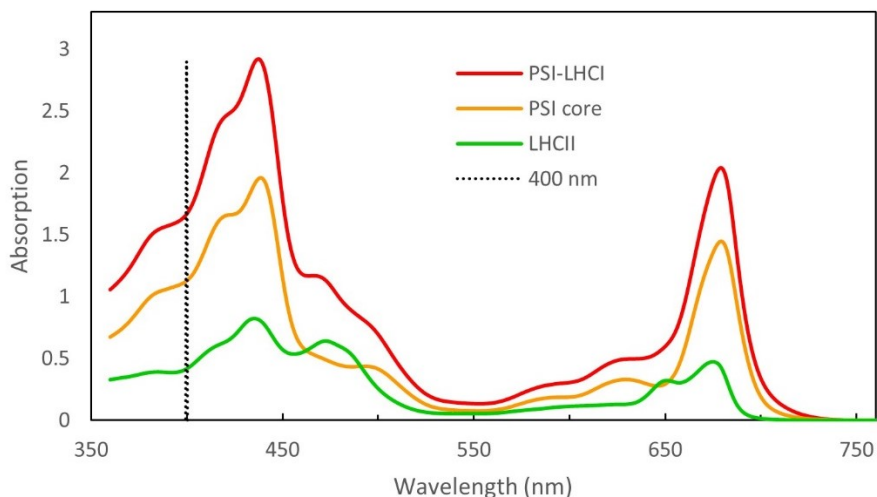


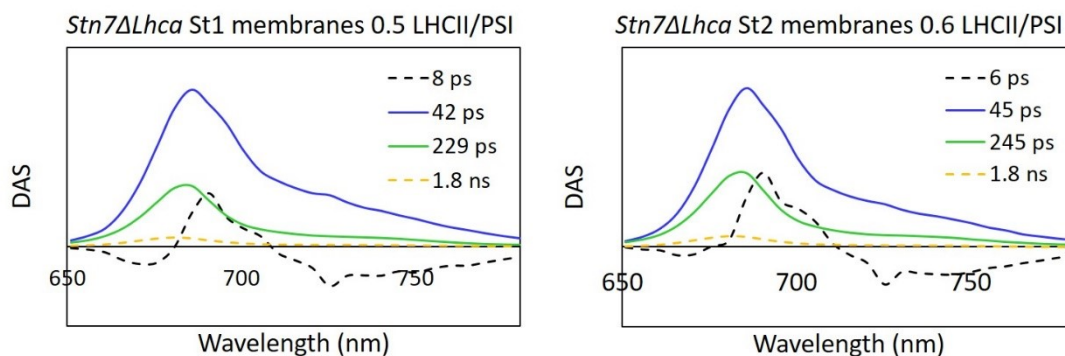
Supplementary Information with
"The role of LHCI in excitation-energy transfer from LHCII to photosystem I in *Arabidopsis*".

Christo Schiphorst, Luuk Achterberg, Rodrigo Gómez, Rob Koehorst, Roberto Bassi, Herbert van Amerongen, Luca Dall'Osto, Emilie Wientjes

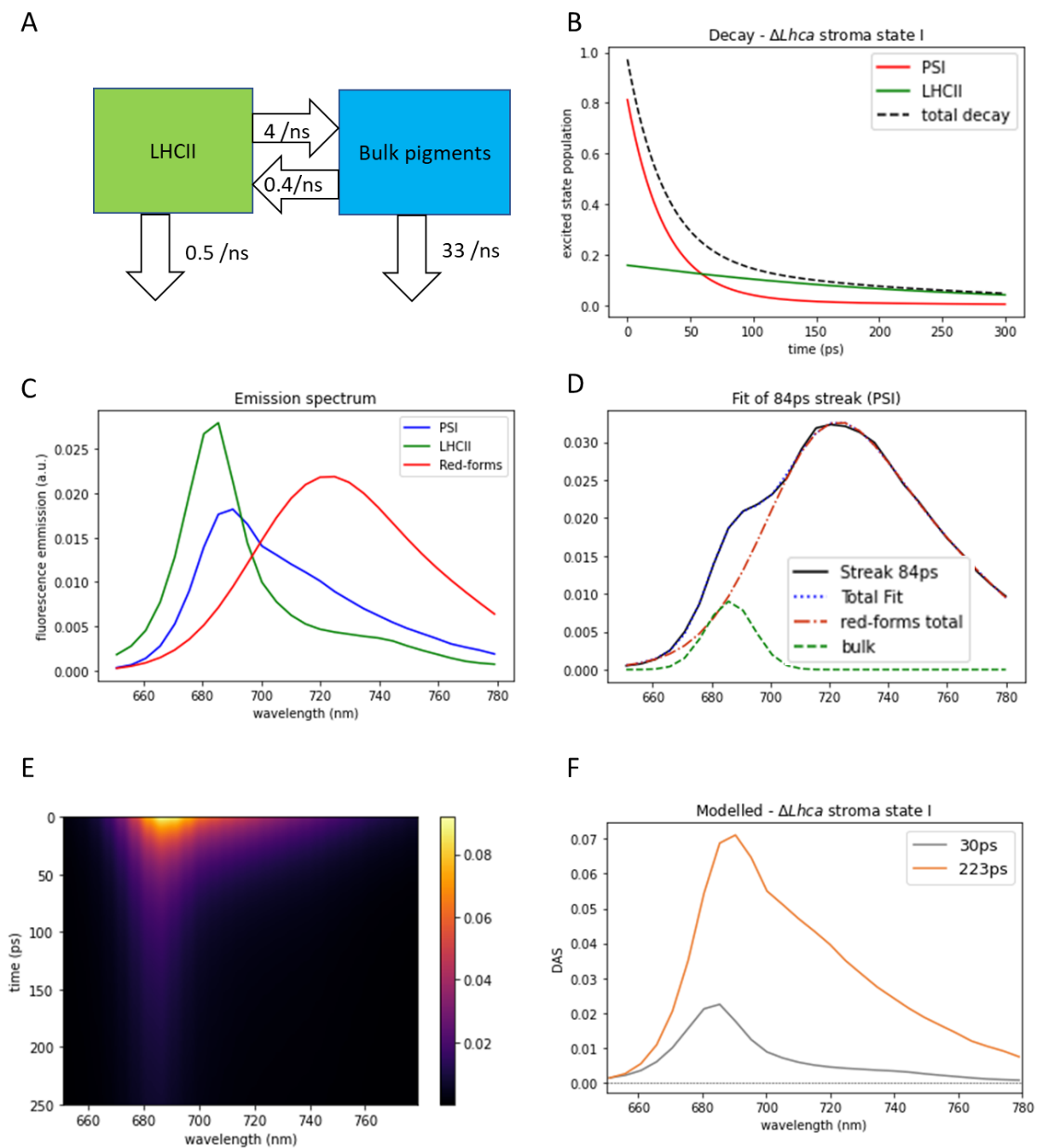
Figures



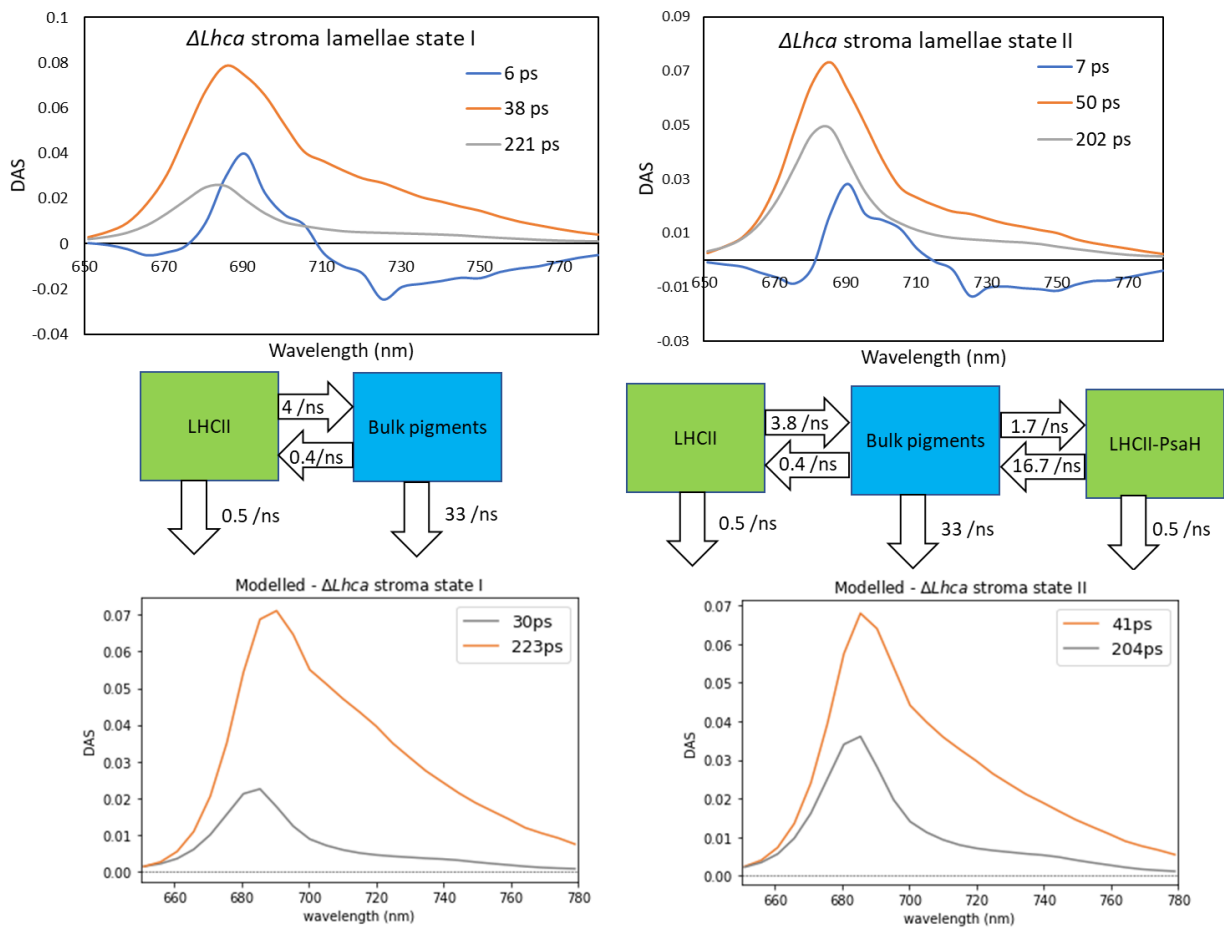
Supplemental Figure S1. Absorption spectra of PSI-LHCI, PSI core and LHCII trimer. Spectra are normalized to the number of chlorophylls per complex as described in Materials and Methods. The excitation wavelength of 400 nm, used for the streak measurements, is indicated.



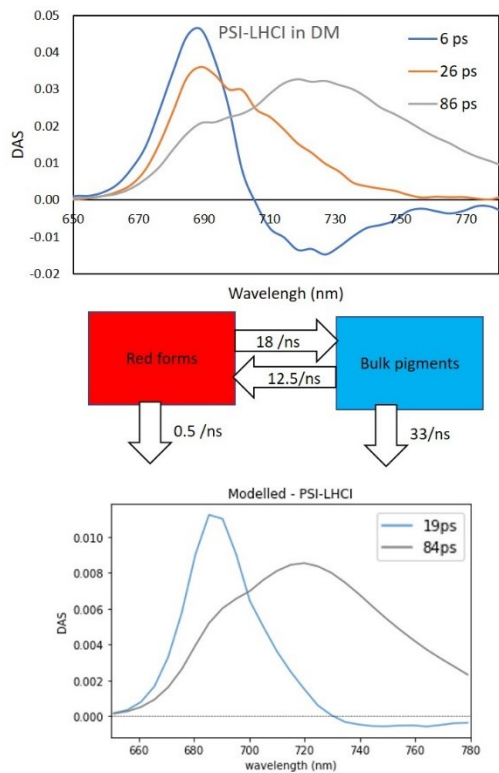
Supplemental Figure S2. Decay associated spectra (DAS) of *Stn7ΔLhca* stroma lamellae membranes. Excitation was at 400 nm. The number of LHCII complexes per PSI, based on the SDS-PAGE analysis, is indicated in the Figure.



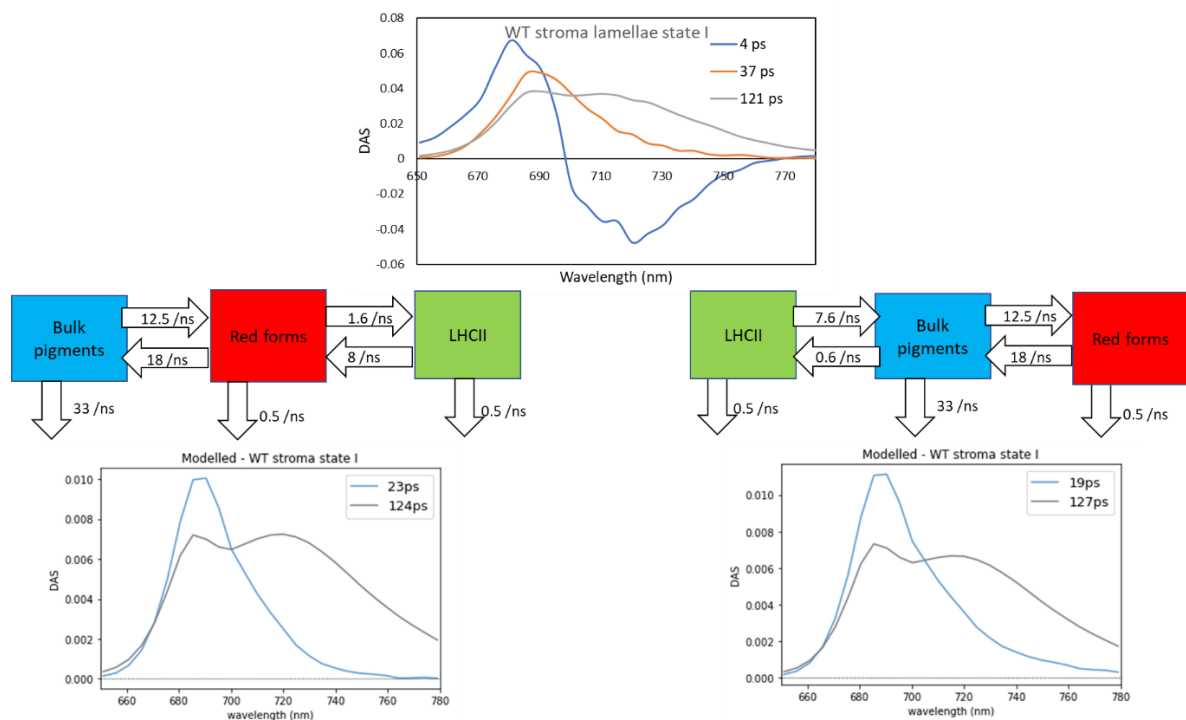
Supplemental Figure S3. Kinetic modelling approach. A. Minimal kinetic scheme for the State 1 $\Delta Lhca$ stroma lamellae membranes. B. The excited state population of LHCII and PSI core is calculated based on the minimal model. C. Fluorescence emission spectra of: LHCII, PSI core (or PSI core + bulk LHCI pigments of LHCI), red forms of LHCI. D. The spectrum of the red forms is derived from the 84 ps DAS of the PSI-LHCI sample where the emission of the bulk Chls *a* is described by a Gaussian shape and subtracted. E. Based on the excited state population and emission spectra the 3D map of the fluorescence intensity as function of wavelength and time is calculated. F. DAS calculated from the data in Figure E.



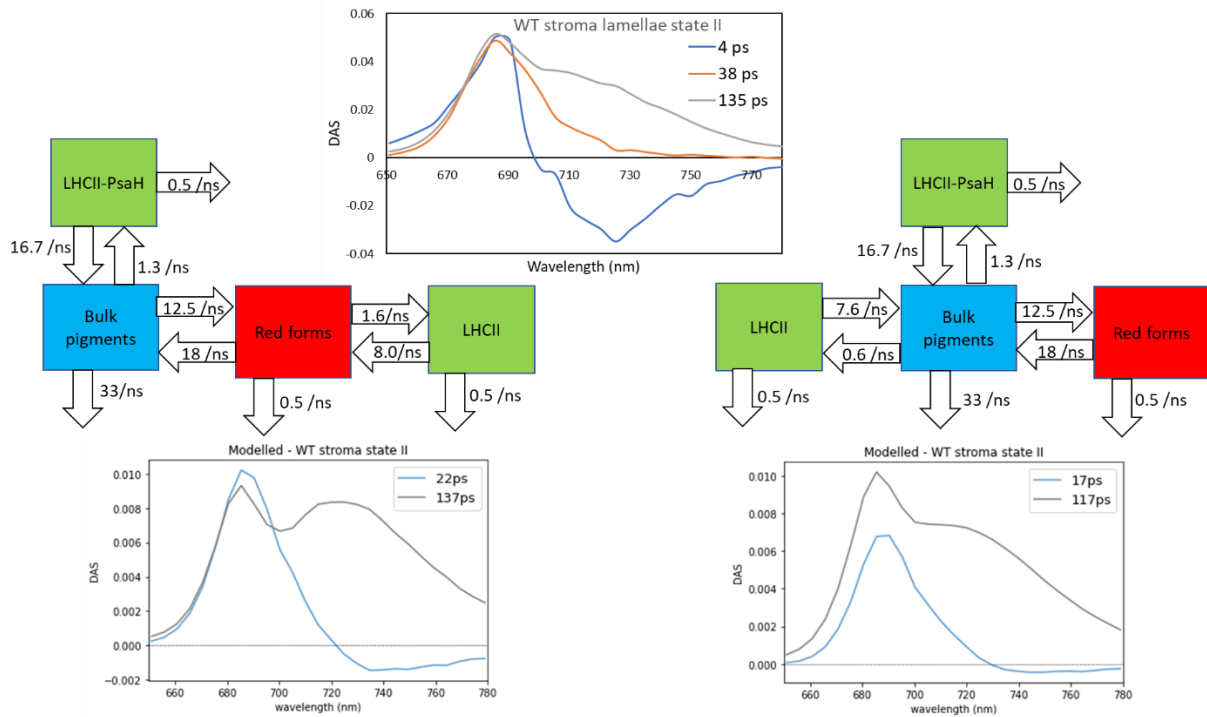
Supplemental Figure S4. Kinetic modelling of $\Delta Lhca$ stroma lamellae excited-state kinetics. The original DAS obtained from the streak measurements are displayed at the top, note that the $\sim ns$ component arising from PSII is omitted. Next the applied minimal models are displayed, followed by the resulting DAS. The model does not include the fast intra-complex energy equilibration between bulk chlorophyll *a* pigments and the few longer wavelength emitting pigments present in the PSI core. As such, the ps equilibration DAS is not reproduced.



Supplemental Figure S5. Kinetic modelling of PSI-LHCI.



Supplemental Figure S6. Kinetic modelling of WT State 1 stroma lamellae excited state kinetics. Two kinetic models are compared. On the right LHCII transfers energy to the bulk chlorophyll a pigments of PSI-LHCI, on the left LHCII transfers energy to the red forms of LHCI. Both models give similar results.



Supplemental Figure S7. Kinetic modelling of WT State 2 stroma lamellae excited state kinetics. The original DAS data (top) is modelled with two schemes. On the left the digitonin sensitive LHCII transfers its energy to the red forms located in LHCI. Instead in the right scheme the energy is transferred to the bulk PSI pigments.

Tables

Supplemental Table S1. Initial excitation of the compartments used for the kinetic modelling. The initial population of the complexes was based on the normalized absorption spectra (Supplemental Figure S1) and the relative abundance of the complexes based on the SDS-PAGE analysis (Table 2 main text). The initial population is considered to be directly related to the absorption of the complex at 400 nm. The red forms are considered to be represented by 4 chlorophylls and therefore taken as 4/155 part of the PSI bulk. A "1" in the table indicates that the compartment is present in the model. Two populations are considered for the stroma lamellae membranes, the relative fractions are indicated in %.

Sample	Fraction	PSI core	PSI bulk	Loose LHCII	PsaH/L/O LHCII	Red forms
	400 nm absorption	1.13	1.63	0.42	0.42	0.04
<i>ΔLhca St1</i>	55%	1		1		
	45%	1				
<i>ΔLhca St2</i>	80%	1		1	1	
	20%	1			1	
WT St1	58%		1	1		1
	42%		1			1
WT St2	64%		1	1	1	1
	36%		1	1		1

Supplemental Table S2. Detailed balance equation for the compartments used for the kinetic modelling. The ratio of downhill and uphill transfer rates is ruled by Boltzmann statistics and described by the detailed balance equation: $\frac{k_{ji}}{k_{ij}} = n_i/n_j e^{-(E_i-E_j)/k_B T}$, with k_{ij} the rate of excitation-energy transfer from pigment pool i to j and k_{ji} the reverse rate, n is the number of chlorophylls a in the pigment pool, E is the energy level of the pigment pool, k_B is the Boltzmann constant and T is the absolute temperature. We used the emission maximum of the pigment pool to calculate the energy level and 293 K as temperature.

Sample	Pigment Pool	Emission max (nm)	Energy (J)	Number of Chl a	$k_{PSI,LHCII}/k_{LHCII,PSI}$
<i>ΔLhca St1</i>	LHCII	682	2.91E-19	24	0.106
	PSI bulk	690	2.88E-19	98	
<i>ΔLhca St2</i>	LHCII	682	2.91E-19	24	0.106
	PSI bulk	690	2.88E-19	98	
PSI-LHCI	Red forms	723	2.75E-19	4	0.74
	PSI bulk	690	2.88E-19	139	
WT St1	LHCII	682	2.91E-19	24	0.075
	Red forms	723	2.75E-19	4	0.74
	PSI bulk	690	2.88E-19	139	
WT St2	LHCII	682	2.91E-19	24	0.075
	Red forms	723	2.75E-19	4	0.74
	PSI bulk	690	2.88E-19	139	

Text

Supplemental Text S1. Kinetic modelling

For all samples a minimal model was used composed of the bulk chlorophyll *a* pigments of PSI (core), LHCII and red forms (Supplemental Figure S3A). The initial populations after excitation at 400 nm were calculated based on the normalized absorption spectra and the relative abundance of the complexes (Supplemental Table S1). Based on the transfer and decay rates, the decay kinetics of the pigment pools was calculated. As an example the kinetic modelling of the State 1 $\Delta Lhca$ mutant (Supplemental Figure S3B) will be described in detail. The results for the other samples were modelled in the same way. The backward and forward transfer rates have to obey the detailed balance relation (Supplemental Table S2). The emission spectra of LHCII and the PSI core (Supplemental Figure S3C) were obtained by measuring the isolated complexes on the streak-camera system. The PSI core spectrum was also used for the bulk PSI emission spectrum. The red forms, required to model the wild type PSI-LHCI data, were based on the 84 ps DAS of PSI-LHCI. The shoulder of the bulk chlorophyll *a* pigment emission was fitted with a Gaussian curve and the rest was assigned to the emission of red forms (Supplemental Figure S3D). The total area under the red forms spectrum was 1.5 times higher compared to the LHCII and PSI (core) spectrum, to account for the higher oscillator strengths of the red forms (Wientjes et al., 2011). Multiplication of the excited-state populations of the PSI core and LHCII with their respective spectra gives the 3D map of the fluorescence intensity as function of time and wavelength (Supplemental Figure S3E). For each wavelength the fluorescence decay kinetics is fitted with a sum of exponentials $F(\lambda, t) = a1 * e^{-\frac{t}{\tau1}} + a2 * e^{-\frac{t}{\tau2}}$, where the lifetimes (τ) are the same for all wavelengths. The amplitudes $a1$ and $a2$ provide the DAS and are plotted in Supplemental Figure S3F. This data is compared to the measured DAS and the transfer rates can be modified to have the best resemblance of both lifetimes and relative heights of the DAS.

Reference

Wientjes E, van Stokkum IH, van Amerongen H, Croce R (2011) Excitation-energy transfer dynamics of higher plant photosystem I light-harvesting complexes. *Biophys J* **100**: 1372-1380